NANO LETTERS

Letter

pubs.acs.org/NanoLett

Resolving Single Plasmons Generated by Multiquantum-Emitters on a Silver Nanowire

Qiang Li,[†] Hong Wei,*[,†] and Hongxing Xu*[,†,‡]

[†]Beijing National Laboratory for Condensed Matter Physics, Institute of Physics, Chinese Academy of Sciences, Beijing 100190, China

[‡]Center for Nanoscience and Nanotechnology, and School of Physics and Technology, Wuhan University, Wuhan 430072, China

Supporting Information

ABSTRACT: Surface plasmons, the collective oscillations of electrons at metal surface, provide the ability to enhance the weak interaction between individual quantum emitters and photons for quantum information applications. The generation of single plasmons by coupling silver nanowire with single quantum emitters opens the prospects of using quantum optical techniques to control single surface plasmons and designing novel quantum plasmonic devices. However, the real applications will deal with multiple plasmons generated from multiple quantum emitters. Here we report the first experimental demonstration of resolving single plasmons generated by a pair of quantum dots (QDs) on a silver nanowire waveguide. The accurate positions of the two QDs with separation ranging from micrometers to 200 nm within the diffraction limit are determined by using super-resolution imaging method. The efficiency of plasmon generation due to the exciton−plasmon coupling is obtained for each QD. Our research takes a crucial step toward the experimental study of coupled systems of multiple quantum emitters and plasmonic waveguides and would shed new light on the study of light-matter interactions for potential quantum optics and quantum information applications.

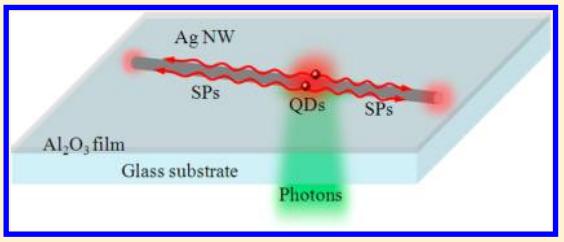

KEYWORDS: *Quantum dot, silver nanowire, surface plasmons, super-resolution imaging, single photon source*

The coupling between individual quantum emitters and photons is a crucial issue for realizing quantum information processing tasks. The cavity quantum electrodynamics has been proposed to address this issue.[1−4] Meanwhile, nanostructures supporting surface plasmons (SPs) can be used to enhance the light-matter interactions.[5−8] Surface plasmon waveguiding devices have gained great interest in recent years because of their ability to manipulate light at nanoscale overcoming the diffraction limit of light.[9−11] A number of experiments have demonstrated relatively long distance SP transmission in several kinds of proposed waveguides, such as noble metal nanowires (NWs),[12−16] V-groove and Λ-wedge,[17−20] hybrid plasmonic waveguide,[21,22] and so on. In 2006, Chang et al. proposed a method that enables strong, coherent coupling between individual optical emitters and electromagnetic excitations in conducting metal NW as well as nanotip.[23] In such metal NW-emitter coupling systems, studies about exciton−plasmon-photon conversion,[24−26] single plasmon generation,[27−30] and single photon transistor[31] have been reported. Realization of efficient and controllable coupling between quantum emitters and plasmonic waveguides would open the door to many potential applications in quantum information and communication technologies.

Quantum dots (QDs) are bright room-temperature single photon sources with tunable emission spectra, which make them important candidates for quantum devices.[32−34] Additionally, owing to their nanometer size, QDs can act as sensitive probes for studying the interaction between individual quantum emitters and plasmonic nanostructures with high spatial accuracy. Inspired by the experimental demonstration of generating single surface plasmons in metal NWs coupled to QDs,[27] a novel scheme that can generate quantum entangled states in a system of two quantum emitters positioned near a plasmonic waveguide is proposed and investigated theoretically.[35−39] When the single optical plasmons pass through the QD pair-NW system,[38] the interference behaviors in transmission and reflection spectra are obtained and the degree of two-qubit entanglement can vary from unity to zero when the Fano-type transmission spectrum occurs.[37] Considering the potential application of the QD pair-NW structure in the field of quantum information, it is of great importance to study the single surface plasmons generated by a pair of quantum emitters coupled to a plasmonic nanowire. Here, we report the first experimental demonstration of a pair of QDs coupling with a silver NW. The separation between the two QDs we studied is ranging from micrometers to 200 nm within the diffraction limit. The SP-generation efficiency of each QD is derived. Our work demonstrates the realization of resolving single surface plasmons generated by multiple quantum emitters and takes a

Received: March 5, 2014
Revised: May 7, 2014
Published: May 20, 2014

   dx.doi.org/10.1021/nl500838q | *Nano Lett.* 2014, 14, 3358−3363

crucial step toward the experimental study of multiple quantum bits in NW-emitters coupled systems.

The schematic illustration of the sample is shown in Figure 1a. Chemically synthesized Ag NWs of diameter about 80 nm

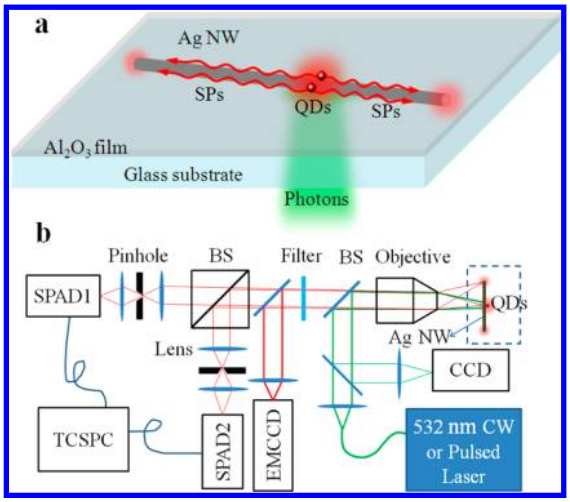

Figure 1. Sample and experimental setup. (a) Sketch of the Ag NW-QD pair system formed by self-assembly. The QDs excited by green laser light generate propagating SPs that couple out as photons at the two ends of the NW. (b) Schematic illustration of the optical setup. BS is a beam splitter. SPAD1 and SPAD2 are two single photon avalanche diodes. TCSPC means a time-correlated single photon counting module.

are deposited on clean cover glass. A spacer layer of 10 nm thickness Al_2O_3 deposited by atomic layer deposition (ALD) method is used to control the separation between the NW and subsequently deposited CdSe/ZnS core/shell QDs. The two QDs located nearby the NW are illuminated by laser light of 532 nm wavelength through an oil immersion objective. Figure 1b shows the sketch of the experimental setup to investigate the QD pair-Ag NW coupling. The emitted fluorescence can be guided to an electron multiplying charge-coupled device (EMCCD) for imaging or to single photon avalanche diodes (SPAD) for measurements of lifetime and second-order photon−photon correlation function (see Supporting Information for more details).

Figure 2 presents the experimental demonstration of a pair of QDs coupling with a Ag NW, where the separation between the two QDs is about 2 μm. Figure 2a shows the photoluminescence (PL) image of the QD pair-NW system taken by EMCCD. When the two QDs A and B were excited simultaneously by the expanded beam of a 532 nm continuous wave (CW) laser, part of the QD energy radiates into free space in the form of photons that are detected as the two large bright spots marked as A and B. Energy from the QDs can also excite the SPs on the NW. During the propagation along the smooth NW, SPs do not couple to observable far field radiations. However, the plasmons on NW can finally scatter out as photons at the ends of the wire as shown by the two smaller bright spots marked as C and D (spectra shown in Supporting Information Figure S3).[26−29]

The coupling of QDs with the NW is also corroborated by the decreased excited state lifetime of these QDs. For an uncoupled QD on substrate, we measured the decay time of its excited state and a single exponential fit yields an excited state lifetime of about 24.2 ns. As a consequence of coupling with the

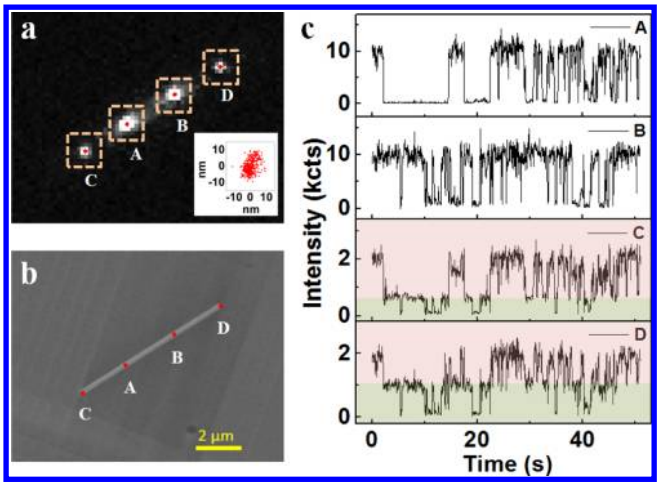

Figure 2. Ag NW coupling with simultaneously excited a pair of QDs. (a) PL image shows the coupling of two QDs with the Ag NW. The bright spots A and B correspond to the QD fluorescence, while the two smaller spots C and D correspond to scattering of SPs at the NW ends. The measured positions of QDs A and B, NW terminals C and D are labeled with red stars. The inset shows the enlarged view of the measured positions of QD A. (b) SEM image of the NW. The diameter of the NW is 113 nm (including the Al_2O_3 layer). The measured positions of QDs and NW ends are overlaid. (c) Time traces of fluorescence counts of QDs A and B and scattered light at the NW ends C and D. The pink area and the cyan area are used to separate the two bright states. The intensity unit kcts means 1000 counts. The light pink squares in (a) show the regions where the counts of each pixel are integrated to generate the emission counts.

NW, the QD feels a changed environment and gets additional recombination channels due to the presence of metal NW,[23] resulting in a reduced excited state lifetime (see Supporting Information Figure S5). For the QDs A and B in Figure 2, the lifetime is 5.6 and 7.7 ns, respectively.

Time traces of fluorescence counts (integrated over the pixels in the light pink squares in Figure 2a) from the QDs A and B are shown in Figure 2c. Clearly, the time trace curves of both QD A and B show a binary blinking behavior, that is, this emitter is randomly switched between ON (bright) and OFF (dark) states under continuous excitation, which is a character of single quantum dot.[40−43] By using a maximum likelihood single molecule localization method,[44−47] the accurate positions of the QDs and the NW terminals are obtained and they are labeled with red stars in Figure 2a. The inset of Figure 2a is the enlarged plot of the measured positions of QD A. The spread range of the measured position is less than 20 nm, consistent with the spatial accuracy of this method which is limited by system noise, fluorescence intensity, magnification, and so on.[45,46] Figure 2b shows the scanning electron microscopy (SEM) image of the NW with the measured positions of QDs and NW terminals labeled with red stars. The accurate distances among the emission spots are as follows: L_{A-C} = 2064 nm, L_{A-B} = 2338 nm, L_{B-D} = 2204 nm. The blinking curves of the scattered photons at C and D show two-level "ON" states, indicating that both QD A and B are efficiently coupled with the NW and they both contribute to the generation of propagating SPs (detailed analysis is given in a later part of this paper).

By using focused laser beam, either of the QDs can be selectively excited. Figure 3 shows the results for selectively exciting each QD. When the QD A was excited by the focused

dx.doi.org/10.1021/nl500838q | Nano Lett. 2014, 14, 3358−3363

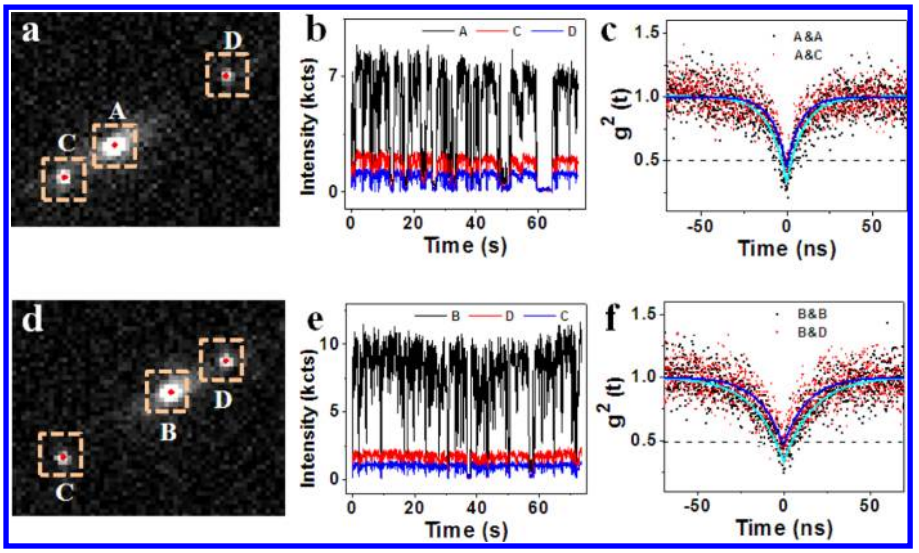

Figure 3. Ag NW coupling with single QD. (a,d) PL images showing the coupling of single QD with the Ag NW. The largest bright spot A (B) corresponds to the QD fluorescence, while the two smaller spots C and D correspond to SPs scattered at the NW ends. The accurate positions of QD A (B), NW terminals C and D are labeled with red stars. (b,e) Time traces of fluorescence counts of QD A (B) and scattered light at the NW ends C and D. The light pink squares in (a,d) show the regions where the counts of each pixel are integrated to generate the emission counts. (c,f) Second-order correlation function $g^{(2)}(t)$ of the QD-NW system. The dots in (c) correspond to the measurements with SPAD1 aligned to emission spot A and SPAD2 to emission spot A (black) or spot C (red) in the PL image shown in (a). The dots in (f) correspond to the measurements with SPAD1 aligned to emission spot B and SPAD2 to emission spot B (black) or spot D (red) in the PL image shown in (d). The cyan (blue) solid lines are exponential fitting of the black (red) dots. The dashed horizontal lines mark the position where $g^{(2)}(t) = 0.5$.

laser, the NW ends lit up (Figure 3a). The large spot corresponds to emission from the QD itself, whereas the two other spots coincide with the wire ends. Significantly, a high degree of correlation was seen between the time traces of the fluorescence counts from the QD and from the ends of the NW (Figure 3b). These observations indicate that the source of the fluorescence from the wire ends is the QD. The single photon and single plasmon excitation are corroborated by measuring the second-order correlation function (antibunching curve) of the emitted light (Figure 3c). The black dots in Figure 3c are for the fluorescence at position A. The low value of $g^{(2)}(0) = 0.29$ confirms the single photon emission from the QD coupled with the NW.[48−50] We also measured the second-order correlation function of the QD fluorescence and NW end emission for which SPAD1 was aligned to emission spot A and SPAD2 to emission spot C (A and C, red dots in Figure 3c). The value of $g^{(2)}(0) = 0.40$ verifies that the light emission at the NW ends is a result of QD-generated single quantized plasmons scattering off the end of the NW.[27−29]

To quantitatively characterize the coupling strength between QD and Ag NW, we define the SP-generation efficiency as the ratio of the QD energy converted to guided SPs and the total energy including both the part converted to SPs and the part radiated to free space (here we do not consider the QD energy damped nonradiatively). This efficiency can be expressed as follows (we assume that the collection efficiency of our detection system for the wire end emission and QD emission is the same)

$$\eta = \frac{I_C e^{\beta L_{A-C}} + I_D e^{\beta L_{A-D}}}{I_A \delta + I_C e^{\beta L_{A-C}} + I_D e^{\beta L_{A-D}}} \quad (1)$$

Here η is the SP-generation efficiency, $I_{C(D)}$ is the intensity of the scattered light at the NW terminal C (D), I_A is the fluorescence intensity of QD A, $1/\beta$ is the propagation length of SPs defined as the length for the plasmon intensity decreased to 1/e of the original intensity, and δ is the transmittance of the NW ends. Here δ is 0.68, which is experimentally obtained (see Section 4 of Supporting Information).[12] On the basis of the assumption that the probability of the energy from the QD going to the two directions is equal, we can relate the propagation length with the intensity of the two wire ends as follows

$$\frac{1}{\beta} = \frac{1}{(L_{A-D} - L_{A-C})} \ln\left(\frac{I_C}{I_D}\right) \quad (2)$$

The ratio of the counts from both ends I_C/I_D is centered at about 1.77 (see Supporting Information Figure S6). By using the above equation, a propagation length of 4362 nm is obtained. This value is quite close to the propagation length obtained by the transmission spectra of NWs with different lengths (see Supporting Information Figure S4), which verifies that the assumption of equal probability for the QD energy going to the two directions is reasonable. The relationship of emission counts at C and A is as follows

$$I_C = \frac{1}{2} I_A \delta \exp(-\beta L_{A-C}) \frac{\eta}{(1-\eta)} \quad (3)$$

We use the time trace at A to fit that at C (see Supporting Information Figure S6) and obtain the SP-generation efficiency of QD A $\eta_A = 0.40$. Using the similar method, we demonstrated the single photon emission of the QD B and the single surface plasmon generation in the NW (Figure 3d–f). The SP-generation efficiency of QD B is about $\eta_B = 0.32$ (see Supporting Information Figure S7). The difference of SP-generation efficiency between QD A and QD B might be from the slight difference in the QD-NW separation or QD orientation.

The SP-generation efficiency of these two QDs can also be obtained when both of them are simultaneously excited as

dx.doi.org/10.1021/nl500838q | Nano Lett. 2014, 14, 3358−3363

shown in Figure 2. The scattering counts at C and D can be expressed as

$$I_C = \frac{1}{2} I_A \delta \exp(-\beta L_{A-C}) \frac{\eta_A}{(1-\eta_A)} + \frac{1}{2} I_B \delta \exp(-\beta L_{B-C}) \frac{\eta_B}{(1-\eta_B)}$$

$$I_D = \frac{1}{2} I_A \delta \exp(-\beta L_{A-D}) \frac{\eta_A}{(1-\eta_A)} + \frac{1}{2} I_B \delta \exp(-\beta L_{B-D}) \frac{\eta_B}{(1-\eta_B)} \quad (4)$$

The weights of contributions from the two QDs are dependent on both the QD positions and their SP-generation efficiency. On the basis of the time traces of fluorescence counts at A and B, we used three free parameters η_A, η_B, and β to fit the time trace recorded at terminal C. The fitting result is $\eta_A = 0.39$, $\eta_B = 0.31$ and $1/\beta = 4634$ nm (see Supporting Information Figure S8). The values of SP-generation efficiency are nearly the same as that fitted from selectively excited QD, which indicates the emission counts at the NW ends result from independent contributions from QDs A and B.

Further, we studied two QDs with reduced separation distance of about 200 nm. Figure 4a shows the PL image of a pair of QDs (separated within the diffraction limit) coupled with a Ag NW when the QDs were excited by focused laser beam. The large bright spot corresponds to the direct far field emission from the QD pair (A and B). The two small light spots (C and D) result from scattered SPs at the ends of the NW. Time traces of fluorescence counts (integrated over the light pink squares shown in Figure 4a) from the QD pair and scattered photons at the ends of the NW are shown in Figure 4c. As can be seen, there are two fluorescence "ON" levels, corresponding to one QD (lower level) and both QDs (upper level) being in the "ON" state, indicating two QDs with similar emission intensity being present. This judgment is also supported by our autocorrelation measurement of the fluorescence from the QD pair ((A and B) and (A and B), black dots in Figure 4d). The number of QDs in the detection area can be estimated by using the normalized correlation function[51,52]

$$g^{(2)}_{\text{normal}}(t) = 1 - \frac{1}{1 + p(N-1) + 2\rho + \frac{1}{Np}\rho^2} e^{-|t|/\tau} \quad (5)$$

where p is the probability to find the QDs in the "ON" state, ρ is the ratio of background intensity to signal intensity for a single QD, N is the number of QDs, $\tau = k_A k_E/(k_A + k_E)$ (k_A and k_E are the absorption and emission rates, respectively). Estimating $p = 0.8$ from the measured time traces of single QDs and the background to signal ratio $\rho = 0.1$ in our experiments, we fit the experimental correlation result by eq 5 with the fitting result shown by the cyan curve in Figure 4d. The fitted number of QDs is 2.25, consistent with our judgment of two QDs based on the time traces of fluorescence counts.

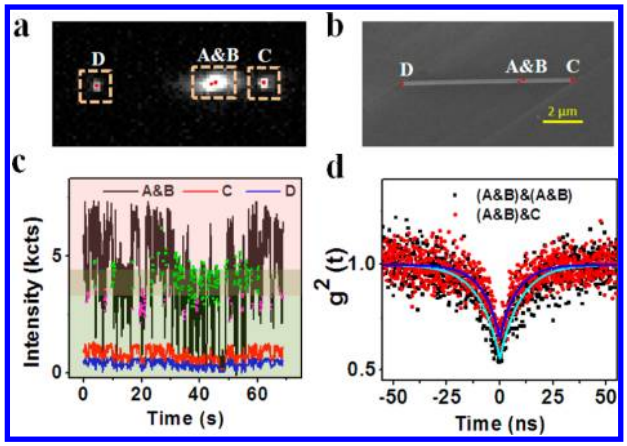

Figure 4. Ag NW coupling with two QDs located in diffraction-limited area. (a) PL image showing the coupling of QDs with the Ag NW. The largest bright spot corresponds to the fluorescence from the two nearby QDs, while the two smaller spots C and D correspond to SPs scattered at the NW ends. (b) SEM image of the NW. The accurate positions of QDs A and B, and NW terminals C and D are labeled with red stars. (c) Time traces of fluorescence counts of QD pair and scattered light at the NW ends. The pink and green dots correspond to the PL images with only QD A or QD B in the bright state. The pink, gray, and cyan areas are used to separate the three bright states. The light pink squares in (a) show the regions where the counts of each pixel are integrated to generate the emission counts. (d) Second-order correlation function $g^{(2)}(t)$ of fluorescence signal for (A and B) and (A and B) (black dots), and (A and B) and C (red dots). The cyan and blue solid lines are fitting results using eq 5 for the black and red dots, respectively.

The second-order correlation function between fluorescence of the QD pair and scattering from the NW end C is shown in Figure 4d ((A and B) and C, red dots). Using eq 5, we obtained a QD number of 2.39, (here we used an increased ratio of background to signal of 0.2 that is mainly caused by the increased fluorescence counts from the Al_2O_3-coated NW and substrate under higher excitation power used to compensate for the low counts from the NW end). This result suggests that the QD-NW coupling process of the two nearby QDs is stand-alone and this conclusion is also supported by the totally unrelated blinking behavior of QD A and QD B.

The time traces of counts at C and D are similar to that of the QD pair (Figure 4c), which means that both of the two QDs are coupled efficiently with the Ag NW. In order to obtain the SP-generation efficiency of each QD, we selected the PL images that clearly show only QD A or QD B (pink dots or green dots in Figure 4c) is in the bright state. By using the maximum likelihood single molecule localization method, the accurate positions of the two QDs and the NW terminals are obtained and they are labeled with red stars in Figure 4a,b. The two spots of fitted QD positions with narrow spread ranges also confirm that there are two QDs. The measured separation distance between the two QDs is 217 nm (see Supporting Information Figure S9). The distances among the emission spots are as follows: $L_{A-D} = 5564$ nm, $L_{B-C} = 2024$ nm. Using the same method as above, we obtain the propagation length of about 4805 nm through the counts ratio between C and D (see Supporting Information Figure S10). The SP-generation efficiencies for the two QDs are deduced from the time traces of emission counts with only QD A in the bright state or only QD B in the bright state. The result is $\eta_A = 0.33$, $\eta_B = 0.28$.

In conclusion, we report the careful analysis of exciton–plasmon coupling between a pair of semiconductor QDs and a chemically grown silver NW. Parameters including the SP propagation length and the wire terminal reflectivity are both experimentally determined and taken into account. By using a super-resolution imaging method, the precise positions of the

dx.doi.org/10.1021/nl500838q | Nano Lett. 2014, 14, 3358–3363

QDs along the NW are obtained, and the separation between two QDs in diffraction-limited area is determined. Our analysis method provides an efficient way to analyze and resolve the coupling of multiple quantum emitters with plasmonic waveguides. For the QD pair-NW system in our study, the two QDs are found independently couple with the NW, and the SP-generation efficiency of the exciton−plasmon coupling is determined for each QD. In another example of a pair of QDs distributed in diffraction-limited area in the proximity of a Ag NW, we show that only one QD is coupled with the NW and generates propagating surface plasmons (see Supporting Information Figure S11), further demonstrating the effectiveness of our analysis method combining super-resolution imaging and time trace correlation. The coupled system of multiquantum-emitters and plasmonic waveguide provides a platform to study quantum optics phenomena and to construct devices of different functions. To explore the entanglement states in this coupled system, the distance between quantum emitters need be precisely controlled because the correlation between two qubits coupled by plasmonic waveguide is dependent on the qubit separation.[35,36]

■ ASSOCIATED CONTENT

Supporting Information

Details about the experimental materials, sample preparation, optical measurements, NW terminal transmittance, and Figures S1−S11. This material is available free of charge via the Internet at http://pubs.acs.org.

■ AUTHOR INFORMATION

Corresponding Authors

*E-mail: (H.W.) weihong@iphy.ac.cn.
*E-mail: (H.X.X.) hxxu@iphy.ac.cn.

Notes

The authors declare no competing financial interest.

■ ACKNOWLEDGMENTS

This work was supported by National Natural Science Foundation of China (Grant Nos. 11134013, 11227407, 11374012, 11004237, and 61210017), The Ministry of Science and Technology of China (Grant Nos. 2012YQ12006005 and 2009CB930700), and "Knowledge Innovation Project" of Chinese Academy of Sciences (CAS) (Grant No. KJCX2-EW-W04). The authors thank the Laboratory of Microfabrication in Institute of Physics of CAS for experimental support.

■ REFERENCES

(1) Imamoglu, A.; Awschalom, D. D.; Burkard, G.; DiVincenzo, D. P.; Loss, D.; Sherwin, M.; Small, A. *Phys. Rev. Lett.* **1999**, *83*, 4204−4207.
(2) Reithmaier, J. P.; Sek, G.; Loffler, A.; Hofmann, C.; Kuhn, S.; Reitzenstein, S.; Keldysh, L. V.; Kulakovskii, V. D.; Reinecke, T. L.; Forchel, A. *Nature* **2004**, *432*, 197−200.
(3) Yoshie, T.; Scherer, A.; Hendrickson, J.; Khitrova, G.; Gibbs, H. M.; Rupper, G.; Ell, C.; Shchekin, O. B.; Deppe, D. G. *Nature* **2004**, *432*, 200−203.
(4) Vahala, K. J. *Nature* **2003**, *424*, 839−846.
(5) Xu, H. X.; Bjerneld, E. J.; Kall, M.; Borjesson, L. *Phys. Rev. Lett.* **1999**, *83*, 4357−4360.
(6) Xu, H. X.; Aizpurua, J.; Kall, M.; Apell, P. *Phys. Rev. E* **2000**, *62*, 4318−4324.
(7) Schuller, J. A.; Barnard, E. S.; Cai, W.; Jun, Y. C.; White, J. S.; Brongersma, M. L. *Nat. Mater.* **2010**, *9*, 193−204.
(8) Tame, M. S.; McEnery, K. R.; Ozdemir, S. K.; Lee, J.; Maier, S. A.; Kim, M. S. *Nat. Phys.* **2013**, *9*, 329−340.
(9) Barnes, W. L.; Dereux, A.; Ebbesen, T. W. *Nature* **2003**, *424*, 824−830.
(10) Maier, S. A. *Plasmonics: Fundamentals and Applications*; Springer: New York, 2007.
(11) Gramotnev, D. K.; Bozhevolnyi, S. I. *Nat. Photonics* **2010**, *4*, 83−91.
(12) Ditlbacher, H.; Hohenau, A.; Wagner, D.; Kreibig, U.; Rogers, M.; Hofer, F.; Aussenegg, F. R.; Krenn, J. R. *Phys. Rev. Lett.* **2005**, *95*, 257403.
(13) Sanders, A. W.; Routenberg, D. A.; Wiley, B. J.; Xia, Y. N.; Dufresne, E. R.; Reed, M. A. *Nano Lett.* **2006**, *6*, 1822−1826.
(14) Wei, H.; Wang, Z. X.; Tian, X. R.; Kall, M.; Xu, H. X. *Nat. Commun.* **2011**, *2*, 387.
(15) Wei, H.; Xu, H. X. *Nanophotonics* **2012**, *1*, 155−169.
(16) Guo, X.; Ma, Y. G.; Wang, Y. P.; Tong, L. M. *Laser Photonics Rev.* **2013**, *7*, 855−881.
(17) Pile, D. F. P.; Gramotnev, D. K. *Opt. Lett.* **2004**, *29*, 1069−1071.
(18) Bozhevolnyi, S. I.; Volkov, V. S.; Devaux, E.; Laluet, J. Y.; Ebbesen, T. W. *Nature* **2006**, *440*, 508−511.
(19) Pile, D. F. P.; Ogawa, T.; Gramotnev, D. K.; Okamoto, T.; Haraguchi, M.; Fukui, M.; Matsuo, S. *Appl. Phys. Lett.* **2005**, *87*, 061106.
(20) Moreno, E.; Rodrigo, S. G.; Bozhevolnyi, S. I.; Martin-Moreno, L.; Garcia-Vidal, F. J. *Phys. Rev. Lett.* **2008**, *100*, 023901.
(21) Oulton, R. F.; Sorger, V. J.; Genov, D. A.; Pile, D. F. P.; Zhang, X. *Nat. Photonics* **2008**, *2*, 496−500.
(22) Liu, N.; Wei, H.; Li, J.; Wang, Z. X.; Tian, X. R.; Pan, A. L.; Xu, H. X. *Sci. Rep.* **2013**, *3*, 1967.
(23) Chang, D. E.; Sorensen, A. S.; Hemmer, P. R.; Lukin, M. D. *Phys. Rev. Lett.* **2006**, *97*, 053002.
(24) Fedutik, Y.; Temnov, V. V.; Schops, O.; Woggon, U.; Artemyev, M. V. *Phys. Rev. Lett.* **2007**, *99*, 136802.
(25) Fedutik, Y.; Temnov, V. V.; Woggon, U.; Ustinovich, E.; Artemyev, M. V. *J. Am. Chem. Soc.* **2007**, *129*, 14939−14945.
(26) Wei, H.; Ratchford, D.; Li, X. E.; Xu, H. X.; Shih, C. K. *Nano Lett.* **2009**, *9*, 4168−4171.
(27) Akimov, A. V.; Mukherjee, A.; Yu, C. L.; Chang, D. E.; Zibrov, A. S.; Hemmer, P. R.; Park, H.; Lukin, M. D. *Nature* **2007**, *450*, 402−406.
(28) Kolesov, R.; Grotz, B.; Balasubramanian, G.; Stohr, R. J.; Nicolet, A. A. L.; Hemmer, P. R.; Jelezko, F.; Wrachtrup, J. *Nat. Phys.* **2009**, *5*, 470−474.
(29) Huck, A.; Kumar, S.; Shakoor, A.; Anderson, U. L. *Phys. Rev. Lett.* **2011**, *106*, 096801.
(30) Falk, A. L.; Koppens, F. H. L.; Yu, C. L.; Kang, K.; Snapp, N. D.; Akimov, A. V.; Jo, M. H.; Lukin, M. D.; Park, H. *Nat. Phys.* **2009**, *5*, 475−479.
(31) Chang, D. E.; Sorensen, A. S.; Demler, E. A.; Lukin, M. D. *Nat. Phys.* **2007**, *3*, 807−812.
(32) Ropp, C.; Cummins, Z.; Nah, S.; Fourkas, J. T.; Shapiro, B.; Waks, E. *Nat. Commun.* **2013**, *4*, 1447.
(33) Zhang, J. T.; Tang, Y.; Lee, K.; Ouyang, M. *Nature* **2010**, *466*, 91−95.
(34) Hennessy, K.; Badolato, A.; Winger, M.; Gerace, D.; Atature, M.; Gulde, S.; Falt, S.; Hu, E. L.; Imamoglu, A. *Nature* **2007**, *445*, 896−899.
(35) Gonzalez-Tudela, A.; Martin-Cano, D.; Moreno, E.; Martin-Moreno, L.; Tejedor, C.; Garcia-Vidal, F. J. *Phys. Rev. Lett.* **2011**, *106*, 020501.
(36) Chen, G. Y.; Lambert, N.; Chou, C. H.; Chen, Y. N.; Nori, F. *Phys. Rev. B* **2011**, *84*, 045310.
(37) Chen, G. Y.; Chen, Y. N. *Opt. Lett.* **2012**, *37*, 4023−4025.
(38) Yang, J.; Lin, G. W.; Niu, Y. P.; Gong, S. Q. *Opt. Express* **2013**, *21*, 15618.
(39) Kim, N. C.; Li, J. B.; Yang, Z. J.; Hao, Z. H.; Wang, Q. Q. *Appl. Phys. Lett.* **2010**, *97*, 061110.

(40) Neuhauser, R. G.; Shimizu, K. T.; Woo, W. K.; Empedocles, S. A.; Bawendi, M. G. *Phys. Rev. Lett.* **2000**, *85*, 3301−3304.
(41) Heuff, R. F.; Swift, J. L.; Cramb, D. T. *Phys. Chem. Chem. Phys.* **2007**, *9*, 1870−1880.
(42) Li, Q. A.; Chen, X. J.; Xu, Y.; Lan, S.; Liu, H. Y.; Dai, Q. F.; Wu, L. J. *J. Phys. Chem. C* **2010**, *114*, 13427.
(43) Galland, C.; Ghosh, Y.; Steinbruck, A.; Sykora, M.; Hollingsworth, J. A.; Klimov, V. I.; Htoon, H. *Nature* **2011**, *479*, 203−207.
(44) Smith, C. S.; Joseph, N.; Rieger, B.; Lidke, K. A. *Nat. Methods* **2010**, *7*, 373−375.
(45) Mortensen, K. I.; Churchman, L. S.; Spudich, J. A.; Flyvbjerg, H. *Nat. Methods* **2010**, *7*, 377−381.
(46) Cang, H.; Labno, A.; Lu, C. G.; Yin, X. B.; Liu, M.; Gladden, C.; Liu, Y. M.; Zhang, X. *Nature* **2011**, *469*, 385−388.
(47) Stranahan, S. M.; Willets, K. A. *Nano Lett.* **2010**, *10*, 3777−3784.
(48) Zwiller, V.; Blom, H.; Jonsson, P.; Panev, N.; Jeppesen, S.; Tsegaye, T.; Goobar, E.; Pistol, M. E.; Samuelson, L.; Bjork, G. *Appl. Phys. Lett.* **2001**, *78*, 2476−2478.
(49) Messin, G.; Hermier, J. P.; Giacobino, E.; Desbiolles, P.; Dahan, M. *Opt. Lett.* **2001**, *26*, 1891−1893.
(50) Kiraz, A.; Falth, S.; Becher, C.; Gayral, B.; Schoenfeld, W. V.; Petroff, P. M.; Zhang, L.; Hu, E.; Imamoglu, A. *Phys. Rev. B* **2002**, *65*, 161303.
(51) Lounis, B.; Bechtel, H. A.; Gerion, D.; Alivisatos, P.; Moerner, W. E. *Chem. Phys. Lett.* **2000**, *329*, 399−404.
(52) Gruber, C.; Kusar, P.; Hohenau, A.; Krenn, J. R. *Appl. Phys. Lett.* **2012**, *100*, 231102.